

The Foam Analogy: From Phases to Elasticity

William Kung

*Department of Physics and Astronomy, University of Pennsylvania, Philadelphia,
PA 19104-6396*

P. Ziherl

*Department of Physics, University of Ljubljana, SI-1000 Ljubljana, Slovenia
J. Stefan Institute, Jamova 39, SI-1000 Ljubljana, Slovenia*

Randall D. Kamien

*Department of Physics and Astronomy, University of Pennsylvania, Philadelphia,
PA 19104-6396*

Abstract

By mapping the interactions of colloidal particles onto the problem of minimizing areas, the physics of foams can be used to understand the phase diagrams of both charged and fuzzy colloids. We extend this analogy to study the elastic properties of such colloidal crystals and consider the face-centered cubic, body-centered cubic and A15 lattices. We discuss two types of soft interparticle potentials corresponding to charged and fuzzy colloids, respectively, and we analyze the dependence of the elastic constants on density as well as on the parameters of the potential. We show that the bulk moduli of the three lattices are generally quite similar, and that the shear moduli of the two non-close-packed lattices are considerably smaller than in the face-centered cubic lattice. We find that in charged colloids, the elastic constants are the largest at a finite screening length, and we discuss a shear instability of the A15 lattice.

1 Introduction

Soft materials are often subjugated into classes: “colloids, polymers, or emulsions”, or “liquid crystals, membranes, or foams”. While these systems all share common mechanical and energetic scales, each subfield has developed its own set of theoretical tools, often required and inspired by real-world applications. Recently [1,2,3] we have combined ideas from these subfields to study colloids which, in addition to the standard excluded-volume interactions, softly

repel each other, either through a surface polymer coating (“fuzzy”) [4] or via a screened Coulomb interaction [5]. While free-volume theory provides remarkably accurate accounting of the free energy of packing the hard cores [6], additional pair interactions are hard to implement analytically to determine in detail the phase behavior of these systems. We have argued that soft repulsion favors larger separations between the colloid surfaces which, in turn, implies that the area of the (mathematical) interface partitioning the Voronoi cells of each colloid should be a minimum [1]. Employing this idea and borrowing from the physics of foams, we have successfully understood the phase diagrams of these and other systems with similar morphologies, *e.g.* dendritic polymers [7], diblock copolymers [8] and star polymers [9]. In this paper we extend this analogy in order to determine the elastic properties of these materials when assembled into three lattices of interest: the face-centered cubic lattice (fcc), which maximizes the packing density of hard spheres [10], the body-centered cubic lattice (bcc), which minimizes the overlap volume of spheres which cover space [11], and the A15 lattice, which is conjectured to minimize the interfacial area of the Voronoi cells [12].

Fortunately, there exists a considerable body of experimental data and facts on many of these colloidal systems: from crystallographic data [13] to charged systems [14,15,16,17] and lyotropic systems [7,18,19]. The abundance of data can be attributed in part to the relative ease of manipulating colloidal systems by chemical means in the laboratory, and the resulting systems can be readily analyzed using optical techniques [13,20,21,22]. In fact, colloidal systems would serve as an ideal experimental playground provided that a recipe exists that would enable predictions of their external mechanical, thermal and electrical properties as functions of internal variables such as the size of colloidal particles and the form of interparticle interaction.

Prior efforts have been made to understand these colloidal systems from first principles. The more traditional routes include molecular dynamics simulations [23] or analytical methods like the density functional approach [24]. While these tools have proven important in our current understanding, they do not provide a robust explanation of the stability of colloidal crystals. Our analogy with the physics of foams provides a unifying explanation of non-close-packed structures in fuzzy colloids and charged polystyrene spheres. In both of these systems the interaction potential consists of a hard core decorated with a “soft”, purely repulsive part. In dendrimers, for instance, the hard core is composed of the aromatic internal part of the micelle-forming conical macromolecules, and the soft corona comes from the interdigitated alkyl chains of the outer part of the micelles [7]. The charged colloids, on the other hand, consist of polystyrene spheres and the soft repulsive tail is their short-range, screened Coulomb potential.

In what follows, we summarize the main concepts behind the foam analogy

in Section II. We see that geometry provides a natural setting to relate the microscopic properties of colloids such as lattice spacing or interparticle interaction to phase diagrams delineating macroscopic and thermal properties of these systems. In section III, we extend this foam analogy to study the elastic properties of these materials by considering small perturbations to the “foams”. Section IV concludes the paper.

2 The Foam Analogy

In this section we sketch the salient features of the mapping between fuzzy colloids and foams. When studying the interactions of spheres, one limit is to treat them as point particles with infinite curvature. Our approach is the other extreme: we treat the interactions between the spheres as if they are between flat, zero-curvature surfaces.

If the system contains only one type of particle, we may divide the volume into equal volume cells, each singly occupied. At fixed density, the volume of the system is the volume of the hard cores and the excess volume of either the salt solution in charged systems or the soft chains within the corona in fuzzy colloids. Since this latter volume can be viewed as enveloping the individual spheres, we imagine breaking the volume up into a lattice of Voronoi cells, each of which contains a colloidal particle. The excess volume can then be written, by definition, as the product of the area of these dividing surfaces and their average thickness. Since the volume of the hard cores and the volume of the whole system is fixed at a given density, the excess volume is also constant and so:

$$A_M d = \text{constant}, \quad (1)$$

where A_M is total area of these bilayers and d is their average thickness. The excess volume depends on the particle density of the system. Using simple geometrical considerations, the volume per particle subtracting the volume of each particle is

$$A_M d = 2 \left(\frac{1}{n} - \frac{\pi}{6} \right) \sigma^3, \quad (2)$$

where $A_M = \gamma^x \sigma^2 n^{-2/3}$, depends on the lattice type ($\gamma^{\text{fcc}} = 5.345$, $\gamma^{\text{bcc}} = 5.308$, $\gamma^{\text{A15}} = 5.288$) and is a dimensionless quantity characterizing the magnitude of area.

Given the repulsive nature of both types of systems, the surfaces of the hard cores within each Voronoi cell would like to be as far apart from one an-

other as possible. Maximizing d to reduce the repulsive interaction amounts to minimizing A_M and we are thus led to consider Kelvin’s problem [25] of partitioning space into equal volume cells having the smallest interfacial area. It follows that the soft repulsion favors the bcc lattice over the fcc lattice [25] and the A15 lattice over both [12,1,7]. The total free energy of the system can be divided into two contributions: a bulk part due to the positional entropy of the hard cores in the Voronoi cells, and an interfacial part due to the surface interactions between neighboring cells. Other than its heuristic nature, the main advantage of our geometrical approach lies in the fact that although it incorporates only nearest-neighbor effects, our calculations have a many-body character since both maximization of the packing density and minimization of the interfacial area are global rather than local problems.

To compute the bulk free energy of the system, we employ cellular free-volume theory [26,27]. In this approximation, each particle is confined to a cage formed by its neighbors. The free volume available to each particle’s center of mass is the volume of the Wigner-Seitz cell after a layer of thickness $\sigma/2$ (where σ is the hard-core diameter of particles) is peeled off of its faces. Since the volume of the Wigner-Seitz cell depends only on the symmetry of the lattice, the bulk free energy encodes information on the geometry of the system. It turns out that the free volume theory yields good quantitative agreement with available numerical simulations at high densities in spite of its mean-field nature [6]. At lower densities, as long as the shear elastic constants are non-zero, we expect that an “Einstein-crystal” description of the phonon modes should be adequate. Indeed, for the systems in which we are interested, the appropriate moduli are all non-zero in the density regime we are probing [28]: therefore there should be no “soft modes” which might otherwise contribute strongly to collective effects.

The use of the free volume theory results in the following expression for the bulk free energy of the fcc or bcc lattice:

$$F_{\text{bulk}}^x = -k_B T \ln \left(\alpha^x \left(\beta^x n^{-1/3} - 1 \right)^3 \right), \quad (3)$$

where $n = \rho\sigma^3$ is the reduced density and σ is the hard-core diameter of each colloidal particle. The coefficients $\alpha^{\text{fcc}} = 2^{5/2}$ and $\alpha^{\text{bcc}} = 2^2 3^{1/2}$ depend on the shape of the cells, whereas $\beta^{\text{fcc}} = 2^{1/6}$ and $\beta^{\text{bcc}} = 2^{-2/3} 3^{1/2}$ are determined by their size.

The bulk free energy expression for the A15 lattice is slightly more complicated but still amenable to an approximate analytical form [1,2]:

$$F_{\text{bulk}}^{\text{A15}} = -k_B T \left[\frac{1}{4} \ln \left(\frac{4\pi S}{3} \left(\frac{\sqrt{5}}{2n^{1/3}} - 1 \right)^3 \right) + \frac{3}{4} \ln \left(2\pi C \left(\frac{\sqrt{5}}{2n^{1/3}} - 1 \right)^2 \left(\frac{1}{n^{1/3}} - 1 \right) \right) \right]. \quad (4)$$

This formula best agrees with the numerical results obtained within the cellular theory for $S = 1.638$ and $C = 1.381$.

A comparison of Eqs. (3) and (4) shows that the free volume theory predicts that at reduced densities below about $n \approx 0.48$, the A15 lattice of hard spheres should become more stable than the fcc lattice, which is physically inadmissible. However, this is not essential since a pure hard-core system melts at reduced densities below $n \approx 1$. We note that this anomaly is not an artifact of the approximations behind Eq. (4); instead, it provides us with a conservative estimate for the range of validity of the cellular theory in this system.

The interfacial free energy of the system, on the other hand, incorporates the specific nature of interparticle interactions at the microscopic level. For charged systems, the interaction is the screened Coulomb potential. As in Ref. [3], the Debye-Hückel approximation and a Derjaguin-like approximation are both used to obtain the interfacial free energy:

$$F_c = 64A_M k_B T n_b \kappa^{-1} \tanh^2 \left(\frac{1}{4} \Psi_s \right) \exp(-\kappa d). \quad (5)$$

where n_b is the bulk counterion number density, Ψ_s is the dimensionless surface potential of colloids, n is the colloid density, and the Debye screening length is $\kappa^{-1} = \sqrt{\epsilon \epsilon_0 k_B T / 2e^2 Z^2 n_b}$, itself a function of these control variables (where $\epsilon \epsilon_0$ is the dielectric constant).

For fuzzy colloids, an argument based on Flory theory of the highly compressed polymer brushes [1,2] yields:

$$F_{\text{surf}} = \frac{\ell N_0 k_B T}{h} = \frac{2\ell N_0 k_B T}{d}, \quad (6)$$

where ℓ is a parameter with the dimension of length that determines the strength of repulsion, N_0 is the number of alkyl chains per micelle, and h , the thickness of the corona, is half the average thickness of the interdigitated matrix of the chains, d . In both systems, maximization of surface spacing d implies the minimization of the interfacial area A_M . From Eq. (2), the density of particles enter directly into the energies of the system through the minimal-area constraint. However, the functional dependence on the particle density differs between them: for the charged colloids, we have a short-range exponen-

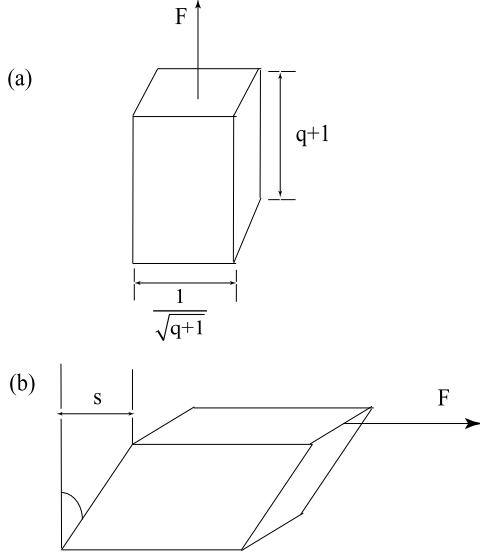


Fig. 1. The two different types of deformations: (a) elongational shear mode; shear deformation along the four-fold axis (b) simple shear mode; shear deformation along the face diagonal. In both cases, we only consider deformations which preserve the total volume of the unit cell. The elongational shear mode is parametrized by q , while the simple shear mode is parametrized by s .

tial interaction while for the fuzzy colloids we have an algebraic interaction, valid at ranges smaller than the thickness of an uncompressed coronal brush.

The bulk and interfacial free energies together express the thermodynamics of colloidal systems in a geometrical language. The formalism directly establishes relations between microscopic parameters governing the dynamics of the colloidal particles and the stability of various macroscopic phases with respect to temperature [3,?]. One can conceivably adapt Eqs. (3), (4), (5), and (6) to other kinds of lattice geometry, and the foam analogy can correspondingly be applied to studying the various solid phases of colloidal systems. In the following section we will consider lattices which can be attained through shearing the fcc, bcc and A15 lattices.

3 From Phases To Elasticity

In general, the elastic energy of a crystal with cubic symmetry has three distinct elastic constants, K_{11} , K_{12} , and K_{44} [29]:

$$F_{\text{cubic}} = \frac{1}{2} \int d^3x \left[K_{11} (u_{xx}^2 + u_{yy}^2 + u_{zz}^2) \right]$$

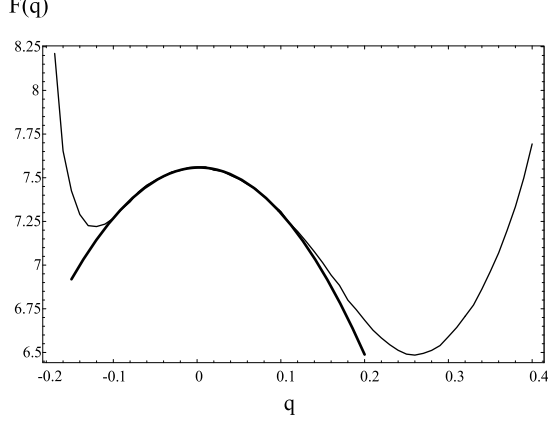


Fig. 2. The bulk free energy of the bcc lattice as a function of the elongational shear at $n = 1.1$. The thick line represents the quadratic fit to the curve at $q = 0$ which determines the bulk part of the shear modulus. The minimum at $q \approx 0.26$ corresponds to the fcc lattice.

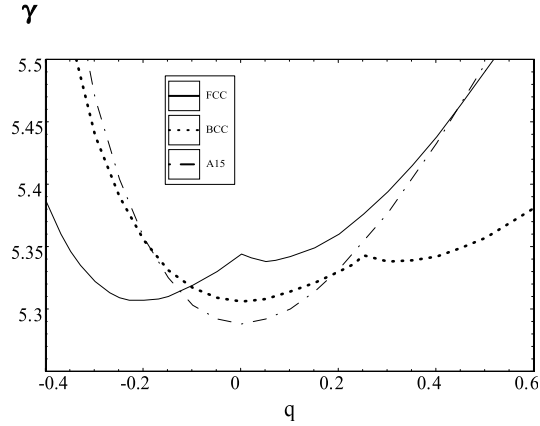


Fig. 3. The surface area parameter γ as function of dimensionless parameter q for the elongational shear mode. The kinks in the curves indicate a change in the topology of the unit cell.

$$\begin{aligned}
 &+K_{12} (u_{xx}u_{yy} + u_{xx}u_{zz} + u_{yy}u_{zz}) \\
 &+2K_{44} (u_{xy}^2 + u_{xz}^2 + u_{yz}^2) \Big]. \quad (7)
 \end{aligned}$$

The bulk modulus $K = \frac{1}{3}(K_{11} + K_{12})$ is an isotropic quantity. The shear modulus, on the other hand, generally depends on the direction of the applied strain and ranges from deformations along the four-fold axis (elongational shear), $\mu = K_{11} - \frac{1}{2}K_{12}$, to deformations along the face diagonal (simple shear), K_{44} . To determine the bulk modulus as well as the three elastic constants, we calculate the changes both in the free volume and in surface area associated with the deformations of the lattice in question (Fig. 1).

The bulk modulus can be expressed in terms of the total free energy of the

system via:

$$K = V \left(\frac{\partial^2 F}{\partial V^2} \right)_T = \frac{1}{3} (K_{11} + K_{12}), \quad (8)$$

where V is the volume of the crystal. To compute the three elastic constants K_{11} , K_{12} , and K_{44} for the fcc, bcc, and A15 lattices in our study, we need two more measurements which we attain from the elongational and simple shear modes.

The elongational shear mode, parametrized by the coordinate transformation $(x, y, z) \rightarrow (x/\sqrt{1+q}, y/\sqrt{1+q}, (1+q)z)$ where $q \ll 1$, induces a corresponding strain $(u_{xx}, u_{yy}, u_{zz}) = (-q/2, -q/2, q)$. Upon substitution into Eq. (7), we find:

$$F_{\text{elong}}(q) = \frac{3V}{4} \left(K_{11} - \frac{1}{2}K_{12} \right) q^2 \quad (9)$$

The volume V simply results from the integration over the free cellular volume in the definition of the elastic free energy. Similarly, the simple shear mode, parametrized by the coordinate transformation $(x, y, z) \rightarrow (x, y, sx + z)$, induces the corresponding strain $u_{xz} = s/2$; all other components of the strain tensor vanish. Analogously, we have:

$$F_{\text{simple}}(s) = \frac{V}{4} K_{44} s^2. \quad (10)$$

The left-hand side of Eqs. (9) and (10) can be found within our framework. There are two contributions from the bulk and interfacial parts: we now find their dependence on the deformation parameters q and s . For example, we consider the elastic energy of the elongational shear of the bcc lattice in Fig. 2. Note that the magnitude of these negative contributions to the bulk modulus increases with increasing density.

The bulk elastic energies can be found via a simple numerical scheme by deforming the unit cell and calculating the resulting free volume of the colloidal particle. At this point, we note that this approach reproduces the well-known shear instability of the bcc lattice of hard spheres. Shear along a four-fold axis, called the Bain strain, reduces the bulk free energy and leads eventually to an fcc lattice via a continuous sequence of body-centered tetragonal (bct) lattices. This is illustrated in Fig. 2 where the bulk free energy of a bcc lattice is plotted as a function of the elongational shear parameter q . At $q = 0$, the unit cell is cubic and the free energy reaches a local maximum. The absolute minimum, which is located at $q = 2^{1/3} - 1 \approx 0.26$ at all densities, corresponds

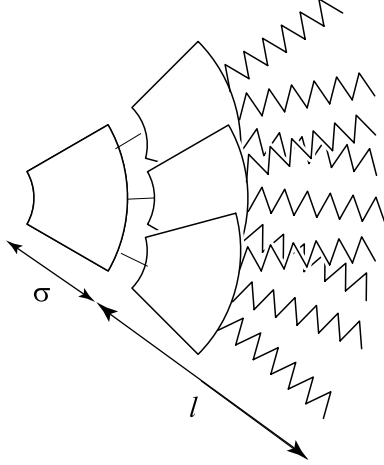


Fig. 4. The effective dimensionless "screening length" of the dendrimers, $L = \ell/\sigma$, corresponds to the ratio of the thickness of the soft outer part, consisting mainly of the alkyl corona, to the radius of the impenetrable hard core of the dendrimer molecule consisting of rigid aromatic rings.

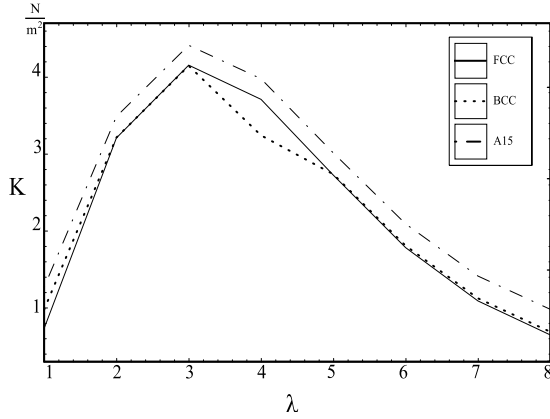


Fig. 5. The bulk modulus K for the fcc, bcc, and A15 lattices of a charged colloidal system as a function of $\lambda = \kappa a$, where a is the average interparticle spacing. The calculations are done at density $n = 0.9$ and at dimensionless surface potential $\Phi_s = 0.4$. The maximum at $\lambda = 3$ is spurious and signals the breakdown of our approximation (see text).

exactly to the fcc lattice. The position of the local minimum at $q < 0$, which describes a bct lattice, depends on density. Its relative depth with respect to the bcc lattice increases with density. The modulus of the curvature near the bcc point increases with increasing reduced density n .

The computation of the interfacial elastic free energy was facilitated by Surface Evolver [30]. Referring to Eq. (2), we can consider the change in γ with respect

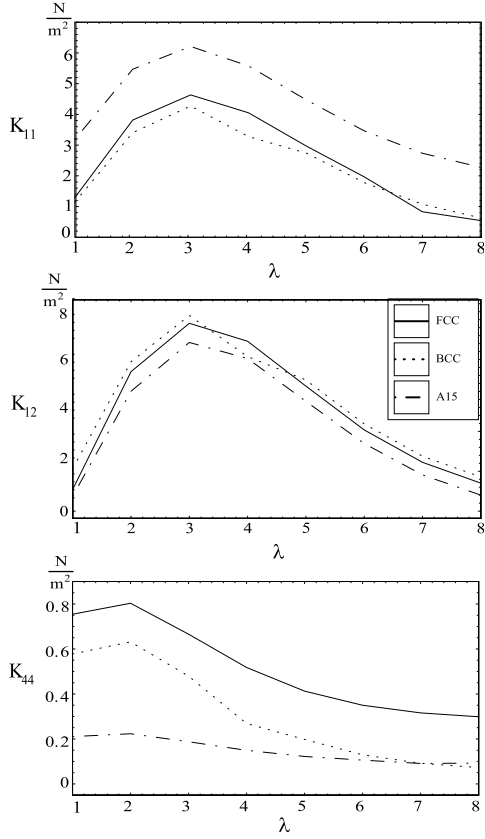


Fig. 6. The elastic constants K_{11} , K_{12} , and K_{44} for the fcc, bcc, and A15 lattices of a charged colloidal system as a function of $\lambda = \kappa a$, at density $n = 0.9$ and at dimensionless surface potential $\Phi_s = 0.4$.

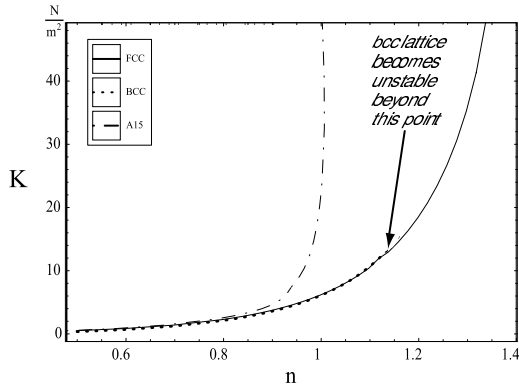


Fig. 7. The bulk modulus K for the fcc, bcc, and A15 lattices of a charged colloidal system as a function of density n , at fixed screening length $\lambda = 4$ and at surface potential $\Phi_s = 0.4$. The bulk modulus K increases with increasing density n for all three lattices and diverges upon close-packing.

to the deformation parameters q and s . This function now encodes the change in surface area of each Voronoi cell under the elongational and simple shear modes, respectively. The numerical result for the elongational shear mode is shown in Fig. 3.

The stability of any particular lattice depends on both the bulk and surface free energy terms. In the bcc lattice, the bulk term favors the shear deformation whereas the surface term does not. It is their relative magnitude that determines whether the lattice is stable, and that depends on density. Since the bulk free energy diverges at close packing, we expect that the bcc lattice should always become unstable at high enough densities. In the following, we only plot the elastic constants for each lattice in the physically relevant range of parameters where the lattice is stable.

We fit the curves shown in Fig. 3 with a quadratic to extract a term proportional to the square of the strain parameter. Upon substitution into Eqs. (5) and (6), we obtain the interfacial contribution to the elastic energy for both the charged and fuzzy colloidal systems, respectively. We repeat the procedure for the set of bulk elastic energy curves (Fig. 2) and the analogous data set for the simple shear mode. The final step requires equating the continuum energy change from Eq. (7) with the calculated energy change and solving numerically for the coefficients in Eqs. (8), (9), and (10).

Some of our results for the case of charged colloids in a bcc lattice have already been reported in Ref. [3]. There we found good agreement with experimental data. Here, we extend our calculations to the fcc and A15 lattices. We also apply this method to the case of fuzzy colloids, of which the fcc and bcc lattices are the main candidates for the solid phase. In each case, we examine the behavior of the bulk modulus as well as the three elastic constants K_{11} , K_{12} , and K_{44} for the three lattices with respect to both varying density and varying effective “screening” length. For charged colloids, the screening length is the Debye screening length κ^{-1} ; the analogous concept for the fuzzy colloid is the corona thickness (Fig. 4).

3.1 Charged Colloids

We first consider the elastic properties of charged colloids. In what follows, the surface potential and the effective diameter of the colloidal particles are chosen to be $\Phi_s = 0.4$ and $\sigma = 910$ nm, respectively. As a function of the screening length at fixed density ($n = 0.9$), the bulk modulus and three cubic elastic constants are shown in Figs. 5 and 6, respectively. Though the elastic constants appear to peak when the interparticle spacing is roughly 3 screening lengths, this is an artifact of our model: as we discussed in [3], when the

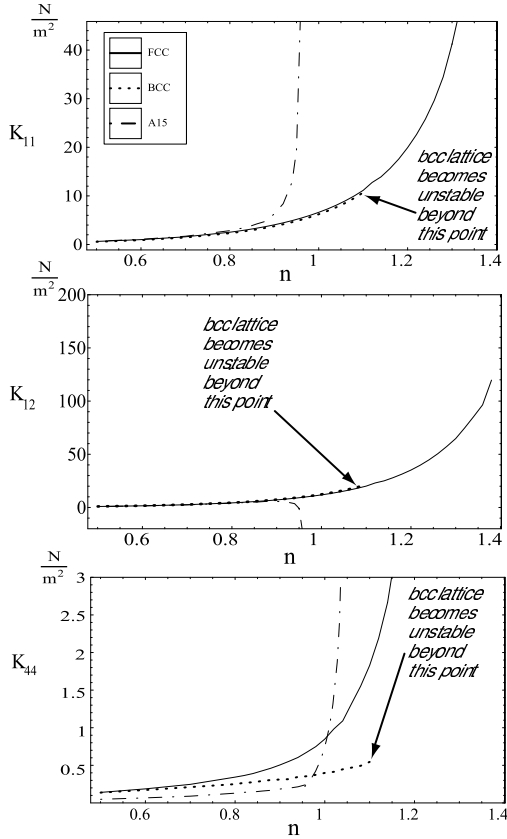


Fig. 8. The elastic constants K_{11} , K_{12} , and K_{44} for the fcc, bcc, and A15 lattices of a charged colloidal system as a function of density n , at fixed $\lambda = 4$ and at surface potential $\Phi_s = 0.4$. Similar to the bulk modulus K , the moduli of the elastic constants diverge upon close-packing.

interparticle spacing, a , is comparable to the Debye screening length, next to nearest neighbor interactions should be included. Since our Derjaguin-like approximation only accounts for nearest neighbors, it is not reliable for $\lambda \equiv \kappa a$ of order 1. Thus we expect that the peaks in the moduli mark the crossover at which the nearest neighbor approximation breaks down. We duplicated the analysis at densities $n = 0.7$ and 0.8 , and we observe the same spurious maximum in the plots of the elastic constants but trust our results beyond the peak.

Next, we consider the elastic constants as functions of varying density at fixed screening length so that $\lambda = \kappa a = 4$ (Figs. 7, 8). Expectedly, the bulk modulus, as well as the three elastic constants K_{11} , K_{12} , and K_{44} , increase with increasing density. Moreover, they diverge upon approaching the close packing limit. We expect this trend to be valid for all other screening lengths as well. The constants K_{11} and K_{12} which control the elongational shear mode have similar magnitudes across different lattices, while the simple shear constant K_{44} is roughly one-tenth of the other two constants, dramatically smaller for

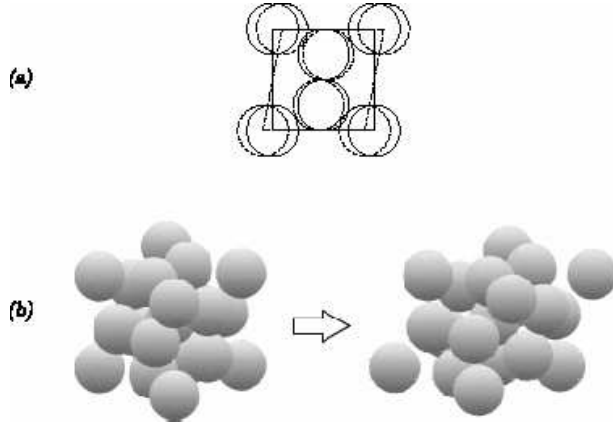


Fig. 9. (a) Schematic of the shear instability of the A15 lattice: the cubic arrangement of the spheres (solid line) is unstable to shear along the face diagonal (dashed line) (b) The cubic A15 lattice and the triclinic derivative lattice as the entropically preferred structure at high densities.

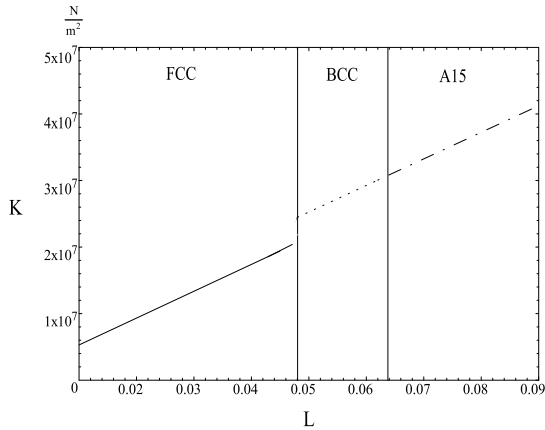


Fig. 10. The bulk modulus for the fcc, bcc, and A15 lattices of a fuzzy colloidal system as a function of "screening" length $L = \ell/\sigma$, at fixed density $n = 0.9$. As the length of the corona increases with increasing L , the thermodynamically favorable structure transits from fcc, to bcc and eventually to the A15 lattice at high enough L . The corresponding bulk modulus simply behaves linearly in the respective regions.

the same systems. It follows that the shear moduli of the charged colloids are considerably smaller than the bulk moduli. If we consider the results for K_{44} , for instance, we see that the modulus is largest in the fcc lattice, and significantly smaller for the A15 lattice. This is similar to the case of hard spheres for which it is well known that the bcc lattice is unstable with respect to shear along the four-fold axis. It is conceivable that for the non-closed packed lattices, there exist pockets of unoccupied space that become available upon shear which would allow an overall lowering of the elastic free energy.

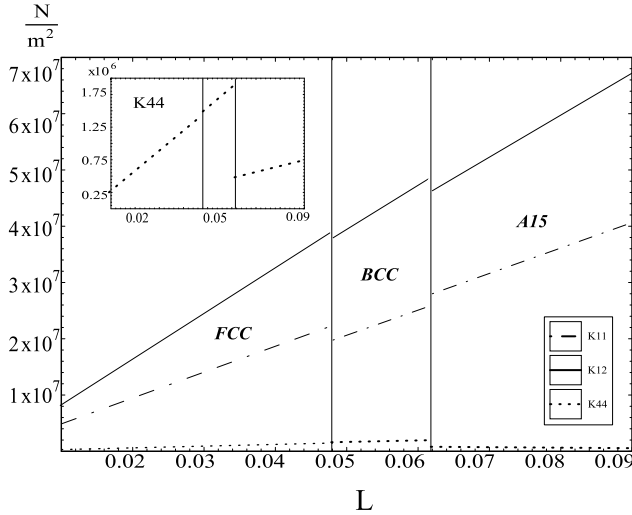


Fig. 11. The elastic constants K_{11} , K_{12} , and K_{44} for the fcc, bcc, and A15 lattices of a fuzzy colloidal system as a function of "screening" length $L = \ell/\sigma$, at fixed density $n = 0.9$. As the "screening" length L increases, non-close-packed structures are favored. Similar to the bulk modulus, the three elastic constants behave linearly with respect to L .

The effects of lattice distortion are less noticeable in the bcc and A15 lattices due to the greater availability of space for each lattice site. Physically, this property translates into the observed fact that the bcc and A15 lattices are much softer and much more amenable to shear deformations. The softening of the bcc shear moduli in comparison to the fcc ones has in fact been seen in MD studies of the fcc lattice of copper [31] and of the bcc lattice of vanadium [32].

In the case of the A15 lattice (Fig. 9), there is an interesting shear mode. This lattice has two distinct sites: pairs of columnar sites are located at bisectors of the faces of the unit cell, forming three sets of mutually perpendicular columns, and interstitial sites are at the vertices and at the center of the unit cell. Fig. 9a shows a side view of the A15 lattice in the close-packing limit, which is determined by the density at which the columnar spheres touch each other—the interstitial sites are still far from their neighbors. There is a shear mode that can exploit this excess volume: consider the deformation shown in Fig. 9a along the $\{110\}$ direction. The sheared lattice (dashed line) is to be contrasted with the cubic close-packing arrangement (solid line). The columnar sites now no longer touch one another, and the free energy is thus lowered in this configuration. However, as the shear increases, the columnar sites touch the interstitial sites and there can be no more distortion. Moreover, since the relative free volume of the columnar and interstitial sites depends on the density, this instability occurs only for a range of densities near the close-packing limit of the A15 lattice; the hard-sphere lattice becomes unstable with respect to shear along the face diagonal at densities greater than $n \approx 0.88$. This is qualitatively different from the shear instability of the bcc lattice,

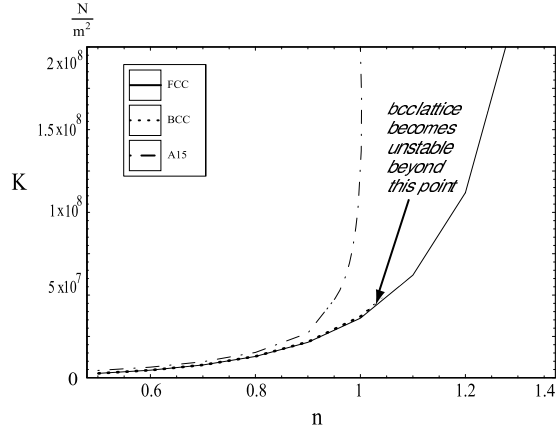


Fig. 12. The bulk modulus K for the fcc, bcc, and A15 lattices of a fuzzy colloidal system as a function of density n , at "screening" length $L = \ell/\sigma = 0.05$. As expected, the bulk modulus K increases with increasing density n .

which is unstable at all densities.

The shear instability shown in Fig. 9a only affects a fraction of all the sites in the unit cell and breaks the symmetry of the cubic lattice, rendering the three columnar sites inequivalent. Since there is no mechanism that would prefer shear along either of the three faces of the A15 unit cell, the actual instability experienced by the system should preserve the equivalence of the columnar sites. Thus it should include equal amounts of shear along all three faces, which corresponds to shear along the body diagonal. The resulting structure belongs to the triclinic system, since the edges of the sheared unit cell are no longer perpendicular to one another. However, the sheared lattice is a special triclinic lattice because the edges of the unit cell are of equal length and the angles between them are identical. It turns out that the angle between the edges which maximizes the packing fraction is $\arccos(1/4) = 75.5$ degrees (Fig. 9b). This configuration gives a packing fraction of 0.5700, to be compared with the A15 packing fraction of $\pi/6 = 0.5236$. Both this instability and the instability of the bcc lattice can be stabilized by the soft repulsion between the colloidal particles, encoded in the surface contribution to the elastic free energy. In both the fuzzy and charged colloidal systems considered in this paper, the parameters of the soft repulsive tail are such that the A15 lattice is stable at all densities considered.

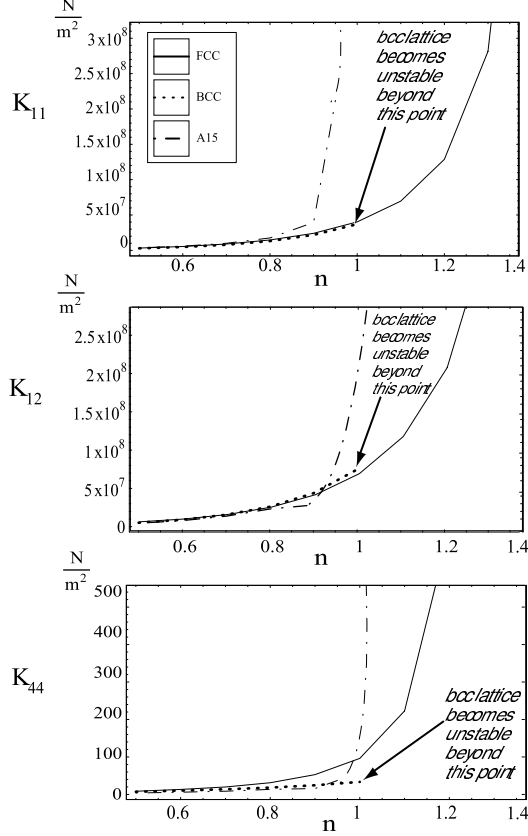


Fig. 13. The elastic constants K_{11} , K_{12} , and K_{44} for the fcc, bcc, and A15 lattices of a fuzzy colloidal system as a function of density n , at "screening" length $L = \ell/\sigma = 0.05$. They increase with increasing density n much like the bulk modulus.

3.2 Fuzzy Colloids

We now turn our attention to fuzzy colloids. As before, we consider the effect of both varying the "screening" length and the density. At a fixed density of $n = 0.90$, we compare the total free energies within the high-density regime as in Ref. [2] and find that the bcc lattice becomes more favorable than fcc at $\ell \approx 0.043\sigma$, whereas the bcc–A15 transition occurs at $\ell \approx 0.062\sigma$. In order to make comparison with the previous study, we will focus on dendrimers with $N_0 = 162$ dodecyl chains per 3rd and 4th generation micelle with a particle size of $\sigma = 4$ nm [7,1]. The bulk modulus and the elastic constants are calculated for each lattice in their respective stability region at fixed density $n = 0.9$ and the results are shown in Figs. 10 and 11. Due to the functional form of the surface energy [Eq. (6)], the linear dependence on $L = \ell/\sigma$ is preserved in the bulk modulus and the three elastic constants. Thus they all vary directly with the screening length. We again observe the trend that K_{44} is smallest for the A15 lattice than for the other lattices, while the overall magnitude of K_{44} is

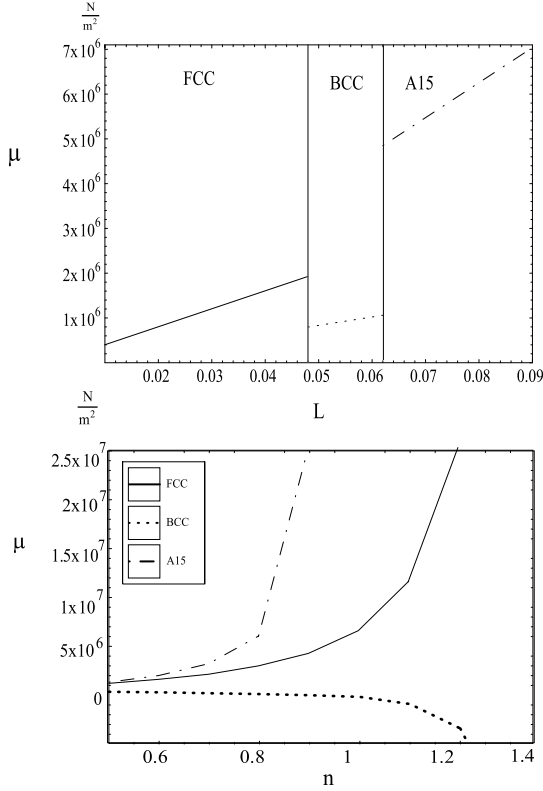


Fig. 14. The shear constants $\mu = K_{11} - K_{12}/2$ for the fcc, bcc, and A15 lattices of a fuzzy colloidal system as a function of density n and "screening" length $L = \ell/\sigma$. They result from the elongational shear mode and represent the lower bound of the average shear measurable in experiments.

less than those of K_{11} and K_{12} . Presumably, the argument presented above for the charged colloids would apply here as well.

At fixed $L = 0.05$, the plots of the bulk modulus and the elastic constants as functions of density are shown in Figs. 12 and 13. Except for K_{12} in the A15 lattice, they all increase with density and diverge upon approaching close packing. The K_{44} values are also smaller than those of K_{11} and K_{12} across the lattices. The elongational shear constants for the non-closed packed structures are consistently smaller than their fcc counterpart, in both systems of fuzzy and charged colloids. (Figs. 14 and 15). As with the charged colloids, the shear modulus of the bcc lattice becomes negative at large enough reduced density in the fuzzy colloids as well; only the physically relevant elastic constants have been included in our plots. In summary, the elastic properties of the fuzzy colloids behave similarly to those of charged colloids, in spite of the overall scaling of the elastic constants. The six orders of magnitude difference between the two systems is simply due to the large difference in the sizes of fuzzy and charged colloidal particles.

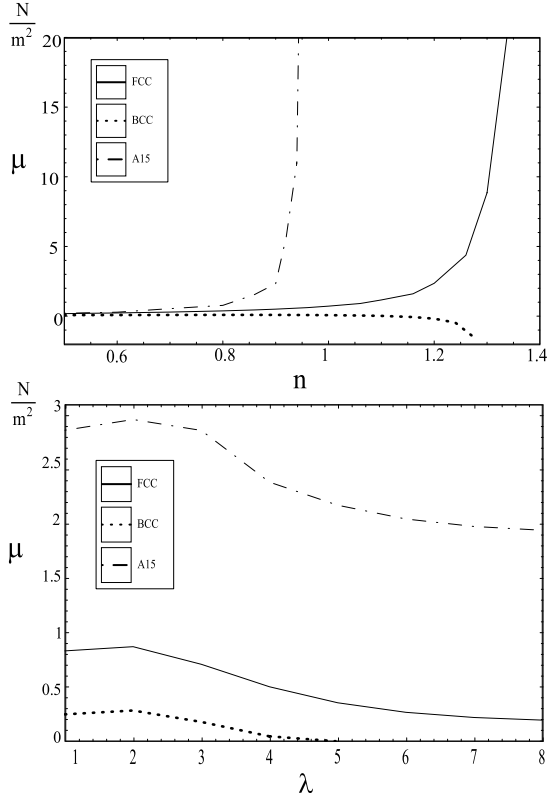


Fig. 15. The shear constants $\mu = K_{11} - K_{12}/2$ for the fcc, bcc, and A15 lattices of a charged colloidal system as a function of density n and $\lambda = \kappa a$. They increase with increasing density, as expected, and are the theoretical lower bound to the range of average shear.

4 Conclusion

In this study, we have used the physical analogy with foams to study the phases of crystalline lattices and their elasticity properties. We find that while the bulk moduli of the lattices considered are quite similar at all densities away from their respective close-packing limits, the relative differences of their shear moduli are much larger. The shear moduli of the non-close-packed lattices are smaller than those of the fcc lattice.

In many ways, the two systems considered are similar, indicating that the details of the interparticle interaction are not essential for all macroscopic properties of colloids. We hope that the foam analogy used here provides an intuitive and mathematically tangible formalism that relates macroscopic properties of colloidal systems directly to their microscopic constituents. Recently, such materials are becoming increasingly important for a range of applications. We are hopeful that our model will serve as a useful guide for further study and synthesis, and, possibly, the engineering of colloidal crystals

of specific geometry and desired properties. Materials with increasingly more complex crystal structures are synthesized [33] and theoretically predicted [34] at an ever growing rate, and their understanding in terms of an heuristic model should prove useful.

5 Acknowledgments

It is a pleasure to acknowledge stimulating discussions with M. Robbins, D. Weitz and T. Witten. This work was supported by NSF Grant DMR01-29804, the Donors of the Petroleum Research Fund, Administered by the American Chemical Society and a gift from L. J. Bernstein.

References

- [1] Ziherl, P. & Kamien, R.D., Soap froths and crystal structures, 2000, Phys. Rev. Lett. 85, 3528–3531.
- [2] Ziherl, P. & Kamien, R.D., Maximizing entropy by minimizing area: towards a new principle of self-organization, 2001, J. Phys. Chem. B 105, 10147-10161.
- [3] Kung, W, Ziherl, P., & Kamien, R.D., The foam analogy in charged colloidal crystals, 2002, Phys. Rev. E 65, 050401-050404 (R).
- [4] Whetten, R.L., Shafigullin, M.N., Khoury, J.T., Schaaff, T.G., Vezmar, I., Alvarez, M.M., & Wilkinson, A., Crystal structures of molecular gold nanocrystal arrays, 1999, Acc. Chem. Res., 32, 397-406.
- [5] Sirota, E.B., Ou-Yang, H.D., Sinha, S.K., Chaikin, P.M., Axe, J.D., & Fujii, Y., Complete phase diagram of a charged colloidal system: a synchrotron X-ray scattering study, 1989, Phys. Rev. Lett. 62, 1524-1527.
- [6] Curtin, W.A., & Runge, K., Weighted density-functional and simulation studies of the bcc hard-sphere solid, 1987, Phys. Rev. A 35, 4755-4762.
- [7] Balagurusamy, V.S.K., Ungar, G., Percec, V., & Johansson, G., Rational design of the first spherical supramolecular dendrimers self-organized in a novel thermotropic cubic liquid-crystalline phase and the determination of their shape by x-ray analysis, 1997, J. Am. Chem. Soc. 119, 1539-1555.
- [8] McConnell, G.A., & Gast, A.P., Predicting disorder-order phase transitions in polymeric micelles, 1996, Phys. Rev. E 54, 5447-5455.
- [9] Beyer, F.L., Gido S.P., Velis, G., Hadjichristidis, N., & Tan, N.B., Morphological behavior of A_5B miktoarm star block copolymers, 1999, Macromolecules 32, 6604-6607.

- [10] Hales, T.C., Cannonballs and honeycombs, 2000, Notices Amer. Math. Soc. 47, 440-450.
- [11] Conway J.H., & Sloane, N.J.A.: *Sphere Packings, Lattices and Groups*, Springer-Verlag (New York, 1999).
- [12] Weaire, D., & Phelan, R., A counterexample to Kelvin's conjecture on minimal surfaces, 1994, Phil. Mag. Lett. 69, 107-110.
- [13] Russel, W.B., Saville, D.A., & Schowalter, W.R., : *Colloidal Dispersions*, Cambridge University Press (New York, 1989).
- [14] Hone, D., Alexander, S., Chaikin, P.M., & Pincus, P.J., The phase diagram of charged colloidal suspensions, 1983, J. Chem. Phys. 79, 1474-1479.
- [15] Kremer, K., Robbins, M.O., & Grest, G.S., Phase diagram of Yukawa systems: model for charge-stabilized colloids, 1986, Phys. Rev. Lett. 57, 2694-2697.
- [16] Rosenberg, R.O., & Thirumalai, D., Order-disorder transition in colloidal suspensions, 1987, Phys. Rev. A 36, 5690-5700.
- [17] Rascón, C., Velasco, E., Mederos, L., & Navascués, G., Phase diagrams of systems of particles interacting via repulsive potentials, 1997, J. Chem. Phys. 106, 6689-6697.
- [18] Percec, V., Ahn, C.H., Ungar, G., Yeardley, D.J.P., Moller, M., & Sheiko, S.S., Controlling polymer shape through self-assembly of dendritic side-groups, 1998, Nature 391, 161-164.
- [19] Hudson, S.D., Jung, H.T., Kewsuwan, P., Percec, V., & Cho, W.D., Grain Boundaries and stacking faults in a Pm3n cubic mesophase, 1999, Liq. Cryst. 26, 1493-1499.
- [20] Hachisu, S., Kobayashi, Y., Takano, K., & Rose, A., Segregation phenomena in monodisperse colloids, 1976, J. Col. Int. Sci. 55, 499-509.
- [21] Yoshiyama, T., Ordering process of colloidal crystal in semidilute aqueous suspensions, 1986 Polymer 27, 828-833.
- [22] Monovoukas, Y. & Gast, A.P., The experimental phase diagram of charged colloidal suspensions, 1989, J. Col. Int. Sci. 128, 533-548.
- [23] Robbins, M.O., Kremer, K., & Grest, G.S., Phase diagram and dynamics of Yukawa systems, 1988, J. Chem. Phys. 88, 3286-3312.
- [24] Sengupta, S. & Sood, A.K., Theory of liquid-bcc-fcc coexistence in charge-stabilized colloidal systems, 1991, Phys. Rev. A 44, 1233-1236.
- [25] Thomson, W., On the division of space with minimum partitional area, 1887, Phil. Mag. 24, 503.
- [26] Hill, T.L.: *Statistical Mechanics*, McGraw-Hill (New York, 1956).
- [27] Barker, J.A.: *Lattice Theory of the Liquid State*, Pergamon Press (Oxford, 1963).

- [28] We thank M. O. Robbins for discussions on this point.
- [29] Chaikin, P.M., & Lubensky, T.C., *Principles of Condensed Matter Physics* Cambridge University Press (New York, 1995).
- [30] Brakke, K., The surface evolver, 1992, Exp. Math. 1, 141-165.
- [31] Kanigel, A., Adler, J., & Polturak, E., Influence of point defects on the shear elastic coefficients and on the melting temperature of copper, Int. J. Mod. Phys. C 12, 727-737.
- [32] Sorkin, V., Polturak, E., & Adler, J., Molecular dynamics study of melting of a bcc metal-vanadium I: mechanical melting, 2003, cond-mat/0304215.
- [33] Ungar, G., Liu, Y., Zeng, X., Percec, V., & Cho, W.D., Giant supramolecular liquid crystal lattice, 2003, Science 299, 1208-1211.
- [34] Likos, C.N., Hoffmann, N., Löwen, H., & Louis, A.A., Exotic fluids and crystals of soft polymeric colloids, 2002, J. Phys. C 14, 7681-7698.